Molecular Crystals and Liquid Crystals
Publication details, including instructions for authors and subscription information:
http://www.tandfonline.com/loi/gmcl20

Precise Dielectric Spectroscopy of a Long Pitch Orthoconic Antiferroelectric Working Mixture

P. Perkowski [a], W. Piecek [a], Z. Raszewski [a], K. Ogrodnik [a], M. Żurowska [b], R. Dąbrowski [b] & J. Kędzierski [a]

[a] Institute of Applied Physics, Military University of Technology, Warsaw, Poland

[b] Institute of Chemistry, Military University of Technology, Warsaw, Poland

Version of record first published: 30 Jun 2011

To cite this article: P. Perkowski, W. Piecek, Z. Raszewski, K. Ogrodnik, M. Żurowska, R. Dąbrowski & J. Kędzierski (2011): Precise Dielectric Spectroscopy of a Long Pitch Orthoconic Antiferroelectric Working Mixture, Molecular Crystals and Liquid Crystals, 541:1, 191/[429]-200/[438]

To link to this article: http://dx.doi.org/10.1080/15421406.2011.569214

Mol. Cryst. Liq. Cryst., Vol. 541: pp. 191/[429]–200/[438], 2011

ISSN: 1542-1406 print/1563-5287 online
DOI: 10.1080/15421406.2011.569214

Taylor & Francis
Taylor & Francis Group

Precise Dielectric Spectroscopy of a Long Pitch Orthoconic Antiferroelectric Working Mixture

P. PERKOWSKI,[1] W. PIECEK,[1] Z. RASZEWSKI,[1] K. OGRODNIK,[1] M. ŻUROWSKA,[2] R. DĄBROWSKI,[2] AND J. KĘDZIERSKI[1]

[1]Institute of Applied Physics, Military University of Technology, Warsaw, Poland
[2]Institute of Chemistry, Military University of Technology, Warsaw, Poland

W-1000 orthoconic antiferroelectric liquid crystal eutectic mixture was prepared in Military University of Technology. This mixture is probably the broadest antiferroelectric mixture, ever prepared. Precise dielectric measurements were performed in a broad temperature range. Some parameters of detected modes and their temperature characteristics are found. It seems that in different temperature regions of orthoconic antiferroelectric liquid crystal different numbers of modes should be anticipated to fit experimental results. Results are discussed with respect to the theoretical model.

Keywords Antiferroelectric mixture; antiferroelectric modes; Cole-Cole equation; Debye model; dielectric relaxation; Goldstone mode

1. Introduction

Orthoconic Antiferroelectric Liquid Crystals (OAFLCs) are very promising materials because of their unique electro-optical behavior [1–3]. These materials are also interesting due to their dielectric properties [4–6]. From theoretical point of view, because of double-layer structure, in planar oriented cell, four collective dielectric modes can be detected in antiferroelectric phase [7] while in Ferroelectric Liquid Crystals (FLCs) two modes can exist [7]. Earlier, in SmC_A^* two modes were observed in many papers, and were called P_L and P_H [8]. The third, ultrafast mode, called X mode was introduced in [9]. This mode, as well as modes P_L and P_H, is highly temperature dependent [10,11]. Relaxation frequency f_R and dielectric strength $\Delta\varepsilon$ change with temperature. For low temperature antiferroelectric phase, forth relaxation is observed in SmC_A^* phase. It seems that this relaxation is faster than X mode. Concerning the theoretical model [7] all four relaxation are explained and new notations are proposed for X mode and for new mode (called "Y mode").

Address correspondence to P. Perkowski, Institute of Applied Physics, Military University of Technology, Warsaw, Poland. Tel.: +48 22 683 95 79; Fax: +48 22 683 92 62; E-mail: pperkowski@wat.edu.pl

2. Experimental

Experiment was done using HP 4192A impedance analyzer, which allows us to perform the measurements from 5 Hz up to 12 MHz. The measuring voltage (AC) was 0.1 V – to avoid non-linear dielectric response, while BIAS voltage (DC) changed from 0 V up to 10 V – to investigate the DC field influence on detected dielectric modes. Measuring frequencies changed from 100 Hz up to 10 MHz. Measuring with frequencies below 100 Hz is useless, because of low accuracy of measurements.

The custom-made measuring cells with golden electrodes were used. Golden electrodes were applied to avoid the high frequency losses related to finite conductivity of ITO electrodes [12–14]. The low resistivity wires were soldered into the cell, with ultrasonic USS-9200 unit. The cell thickness around 5 μm was used to make the alignment good and to avoid creating the untwisted structure. Cell was filled with capillary action in isotropic phase, close to the temperature of I – SmA* phase transition (110°C).

Temperature was controlled using Linkam TMS 92 unit and hot stage Linkam TMSH 660 with accuracy 0.1°C. The sample was slowly cooled, with 0.1°C/min speed. For every temperature, measurements took several minutes. Temperatures below room temperatures were attained using a self-made cooling chamber. Dry ice was used as a coolant. It helps us to reach even −48°C.

The whole experimental setup was controlled by computer, using Agilent Vee software.

3. Investigated Mixture

W-1000 [11] OAFLC mixture was prepared in our University. This is a binary, eutectic mixture, consisting of two slightly different molecules (Fig. 1).

W-1000 shows the following phase sequence:
Cr. (below −23°C) SmC_A^* (100°C) SmC* (103.5°C) SmA* (105.9°C) I
It is, as far as authors know, the broadest antiferroelectric phase ever observed.

4. Results and Discussion

It is well known, that if dielectric losses (ε'') as a function of frequency reach the maximum value, the relaxation frequency can be determined from this peak. In

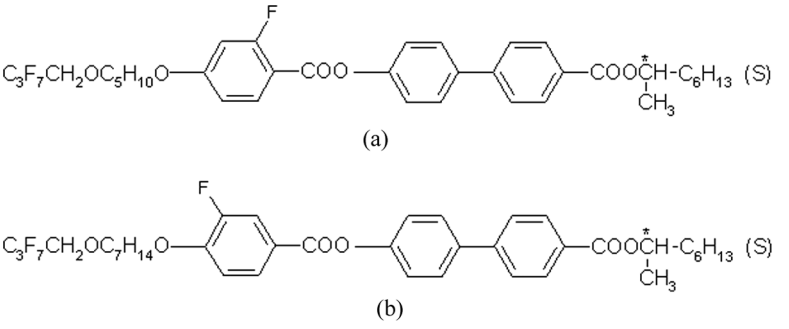

Figure 1. Molecular structure on molecules constituting W-1000 eutectic mixture. 52.52 wt.% of the 1st compound, 48.48 wt.% of the 2nd compound.

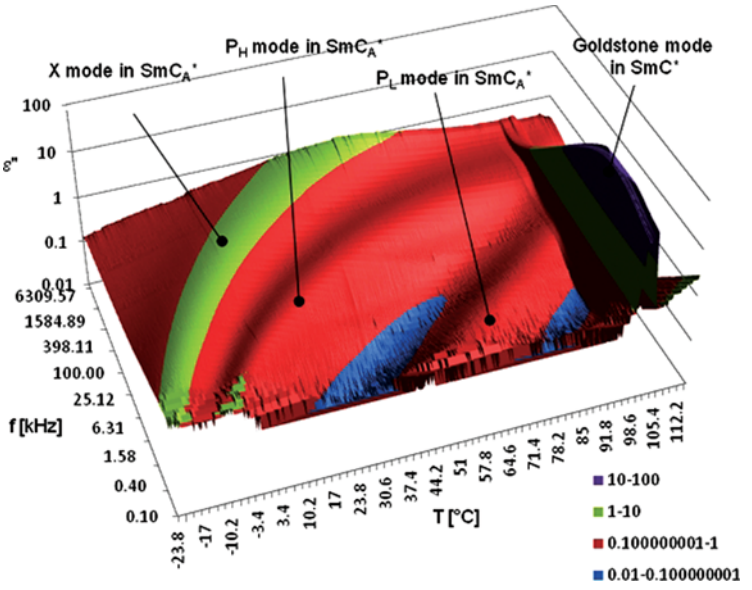

Figure 2. Dielectric losses (ε'') as a function of temperature (T) and frequency (f) for measurements without BIAS voltage. (Figure appears in color online.)

Figure 2 the imaginary part of electric permittivity ε'' is shown in 3D plot as a function of temperature (T) and frequency (f). From this plot one can read the relaxation frequencies of observed modes. It is seen that SmC* phase with large Goldstone mode is detected around 100°C. Below the SmC*, antiferroelectric SmC$_A^*$ appears. In the SmC$_A^*$ three modes are observed unquestionably: low frequency P$_L$, medium frequency P$_H$ and high frequency X modes [9]. In 3D plot it is clearly visible that all three modes relaxation frequencies decrease with temperature decreasing.

This effect is better visible when BIAS field (10 V) is applied to suppress Goldstone mode in SmC*. The results are presented in Figure 3. Now the "gap" in ε'' appears in SmC* phase, where, without BIAS, the strong Goldstone mode is seen in Figure 2. Debye type relaxation interpreted as soft mode is seen close to the temperature of SmA*-SmC* phase transition.

Very interesting is the situation close to SmC*-SmC$_A^*$ phase transition. Three modes are detected in this region: Goldstone, P$_L$ and P$_H$ modes. Figure 4 shows the Cole-Cole [15,16] plots for nine temperatures in this temperature range. It is beyond doubt that Goldstone mode exhibit relaxation frequency below P$_L$ relaxation frequency, while P$_H$ relaxation frequency is higher than for P$_L$.

To find parameters of three detected modes Debye model [17] was used. Experimental results of liquid crystal complex electric permittivity ε_{LC}^* were calculated as a sum of three modes (P$_H$ mode, P$_L$ mode and Goldstone mode):

$$\varepsilon_{LC}^* = \varepsilon'_{LC} - j\varepsilon''_{LC} = \varepsilon_\infty + \frac{\Delta\varepsilon_{PH}}{1 + jf/f_{RPH}} + \frac{\Delta\varepsilon_{PL}}{1 + jf/f_{RPL}} + \frac{\Delta\varepsilon_{GM}}{1 + jf/f_{RGM}}, \qquad (1)$$

where $\Delta\varepsilon_i$ – dielectric strength and f_{Ri} – relaxation frequency for i – mode, ε_∞ – high frequency limit of electric permittivity. We decided to use Debye model because we

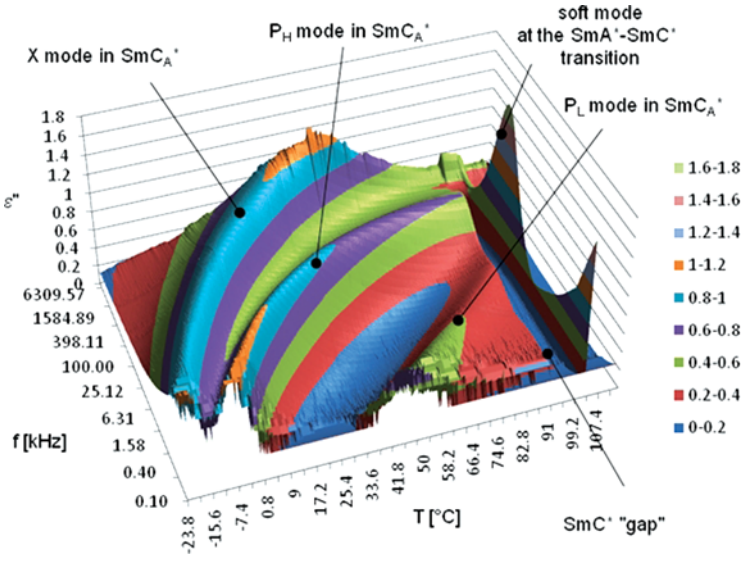

Figure 3. Dielectric losses (ε'') as a function of temperature (T) and frequency (f) for measurements with BIAS voltage (10 V). (Figure appears in color online.)

were assuming the existence of three modes. When we have decided to investigate every mode separately we should use a Cole-Cole model. Cole-Cole model distribution parameter: α, contains the information about neighboring modes, existing close (in frequency domain) to studied mode.

Calculated parameters are collected in Table 1.

It is seen that relaxation frequencies f_{RPH} and f_{RPL} decrease with the temperature decreasing, what is seen also in Figures 2 and 3. The existence of three modes close to SmC*-SmC$_A$* phase transitions is probably because of coexistence of both phases. Relaxation frequency of Goldstone mode slowly decreases when we are entering SmC$_A$* phase. Dielectric strength of Goldstone mode decreases rapidly.

The fitting procedure, performed with MS Excel works very well. Figure 5 shows the fitting results for temperature 95.2°C.

In antiferroelectric phase of W-1000 mixture (close to SmC* phase) two relaxations are detected P_H and P_L. The next interesting situation is close to the

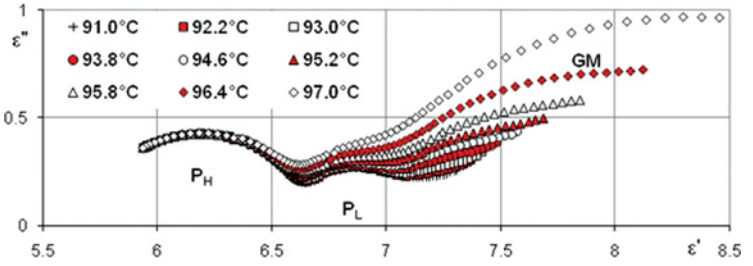

Figure 4. Cole-Cole plots for nine temperatures close to SmC*-SmC$_A$* phase transitions. GM – arc related to Goldstone mode; P_L – arc related to P_L mode; P_H – arc related to P_H mode. (Figure appears in color online.)

Table 1. Three modes fitting parameters, close to SmC*-SmC$_A$* phase transition

T [°C]	ε_∞	f_{RPH} [kHz]	$\Delta\varepsilon_{PH}$	f_{RPL} [kHz]	$\Delta\varepsilon_{PL}$	f_{RGM} [kHz]	$\Delta\varepsilon_{GM}$
97.0	5.908	814	0.7018	38.5	0.4716	2.465	1.651
96.4	5.905	815	0.7070	36.2	0.4517	2.394	1.177
95.8	5.919	802	0.6905	34.3	0.4471	2.332z	0.8920
95.2	5.918	801	0.6944	32.1	0.4405	2.266	0.7396
94.6	5.919	802	0.6949	30.3	0.4391	2.187	0.6224
93.8	5.919	805	0.6978	28.4	0.4346	2.145	0.5239
93.0	5.917	803	0,7040	26.1	0.4356	2.113	0.4375
92.2	5.919	802	0.7077	24.5	0.4328	2.078	0.3844
91.0	5.917	799	0.7176	21.7	0.4366	2.046	0.3331

temperature when P_L mode relaxation frequency is starting to be below measuring range ($f_{RPL} < 100$ Hz) and X mode appears, with very high relaxation frequency ($f_{RXM} \approx 10$ MHz). In Figure 6 dielectric losses (ε'') versus electric permittivity (ε') for 54°C are shown. P_L mode still exists for this temperature and X mode is clearly visible.

The fitting procedure finds three modes parameters to fit experimental values (ε'_{LC} and ε''_{LC}) using Equation 2:

$$\varepsilon^*_{LC} = \varepsilon'_{LC} - j\varepsilon''_{LC} = \varepsilon_\infty + \frac{\Delta\varepsilon_{XM}}{1 + jf/f_{RXM}} + \frac{\Delta\varepsilon_{PH}}{1 + jf/f_{RPH}} + \frac{\Delta\varepsilon_{PL}}{1 + jf/f_{RPL}}, \qquad (2$$

where parameters with XM, PH and PL indexes are related to X mode, P_H mode and P_L mode respectively.

When parameters calculated for plots shown in Figures 5 and 6 are concerned one can notice that P_L mode dielectric strength ($\Delta\varepsilon_{PL}$) slightly increase during cooling. This effect is even stronger for P_H mode. X mode seems to be very fast relaxation in 54°C, and stronger than both relaxations P_H and P_L together.

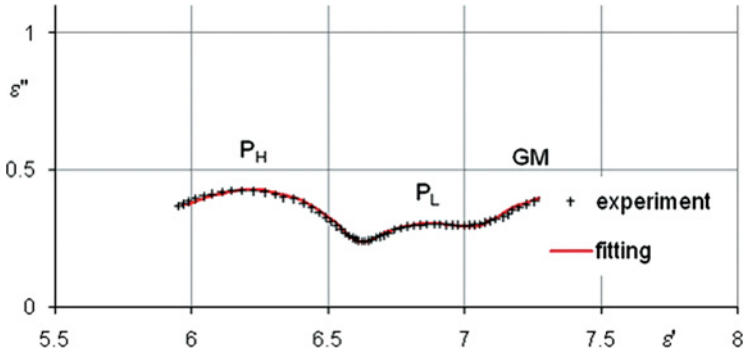

Figure 5. Experimental and fitting results for temperature 95.2°C. Found relaxation frequencies: $f_{RGM} = 2.266$ kHz, $f_{RPL} = 32.1$ kHz, $f_{RPH} = 801$ kHz; dielectric strengths equal: $\Delta\varepsilon_{GM} = 0.7396$, $\Delta\varepsilon_{PL} = 0.4405$, $\Delta\varepsilon_{PH} = 0.6944$; high frequency limit $\varepsilon_\infty = 5.918$. (Figure appears in color online.)

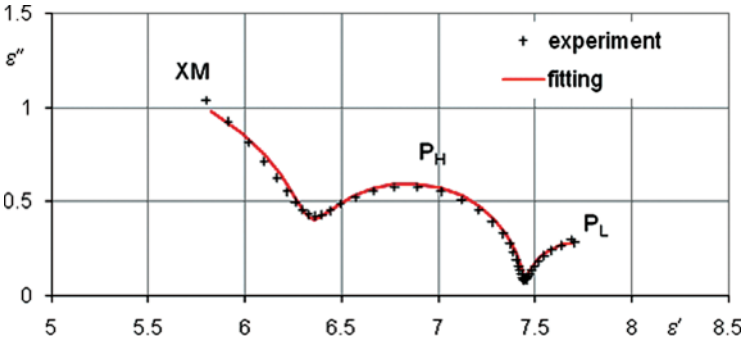

Figure 6. Experimental and fitting results for temperature 54.0°C, where three modes (P_L, P_H and X) exist. Found relaxation frequencies: $f_{RPL} = 0.4576$ kHz, $f_{RPH} = 198.89$ kHz, $f_{RXM} = 11669.81$ kHz; dielectric strengths equal: $\Delta\varepsilon_{PL} = 0.5607$, $\Delta\varepsilon_{PH} = 1.1107$, $\Delta\varepsilon_{XM} = 2.2130$; high frequency limit $\varepsilon_\infty = 4.1201$. (Figure appears in color online.)

When temperature decreases P_L disappears from measuring range. And two modes can be observed: P_H and X mode. It seems that in this case we can apply the fitting procedure presented earlier (Eq. 1 and Eq. 2) but only with two relaxations assumed (Eq. 3):

$$\varepsilon^*_{LC} = \varepsilon'_{LC} - j\varepsilon''_{LC} = \varepsilon_\infty + \frac{\Delta\varepsilon_{XM}}{1 + jf/f_{RXM}} + \frac{\Delta\varepsilon_{PH}}{1 + jf/f_{RPH}}. \qquad (3))$$

Let us to apply this procedure for results collected in room temperature (20°C). The results are presented in Figure 7. It is seen that for room temperature this fitting does not work well. In case of P_H mode fitting works perfectly (it means that this mode is typical Debye mode). X mode seems to be more complicated with more than one relaxation frequency. The Cole-Cole arc is highly asymmetric. Of course in this case we could use another fitting procedure (Havriliak-Negami [18]), which works well for asymmetric arcs. But using computer it is easy to try finding discrete values of relaxation frequencies creating the left arc (Fig. 7). When we assume that X-mode

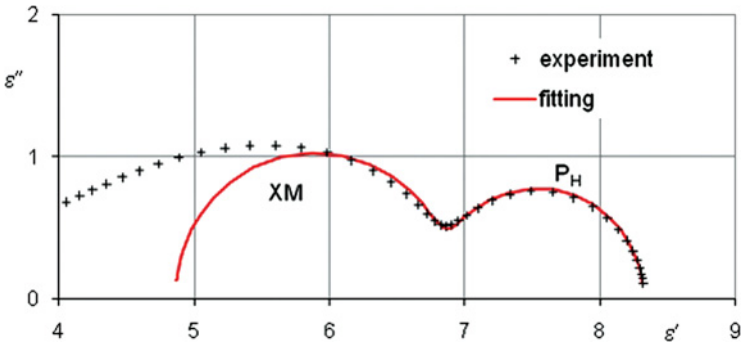

Figure 7. Experimental and fitting results for temperature 20.0°C, where two modes (P_H and X) are expected. Found relaxation frequencies: $f_{RPH} = 10.95$ kHz, $f_{RXM} = 504.7$ kHz; dielectric strengths equal: $\Delta\varepsilon_{PH} = 1.46$, $\Delta\varepsilon_{XM} = 1.99$; high frequency limit $\varepsilon_\infty = 4.8641$. (Figure appears in color online.)

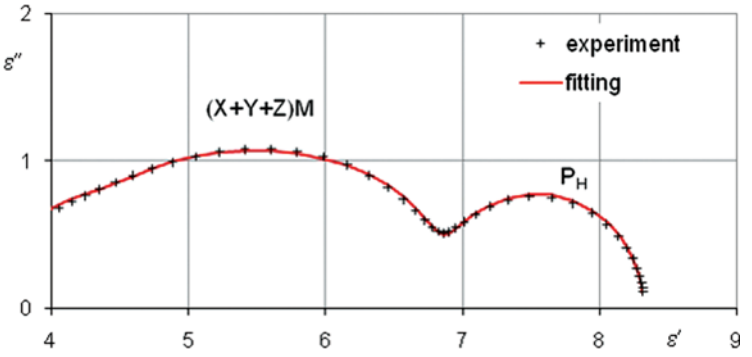

Figure 8. Experimental and fitting results for temperature 20.0°C, where four modes (P_H, X, Y, Z) are assumed. Found relaxation frequencies: $f_{RPH} = 10.91$ kHz, $f_{RXM} = 377.3$ kHz, $f_{RYM} = 1478.0$ kHz, $f_{RZM} = 8946.7$ kHz; dielectric strengths equal: $\Delta\varepsilon_{PH} = 1.46$, $\Delta\varepsilon_{XM} = 1.18$, $\Delta\varepsilon_{YM} = 1.21$, $\Delta\varepsilon_{ZM} = 0.883$; high frequency limit $\varepsilon_\infty = 3.5761$. (Figure appears in color online.)

is the results of three separate modes (X, Y, Z) the fitting (Eq. 4) works much better.

$$\begin{aligned}\varepsilon^*_{LC} &= \varepsilon'_{LC} - j\varepsilon''_{LC} \\ &= \varepsilon_\infty + \frac{\Delta\varepsilon_{ZM}}{1 + jf/f_{RZM}} + \frac{\Delta\varepsilon_{YM}}{1 + jf/f_{RYM}} + \frac{\Delta\varepsilon_{XM}}{1 + jf/f_{RXM}} + \frac{\Delta\varepsilon_{PH}}{1 + jf/f_{RPH}}\end{aligned} \tag{4}$$

The results of fitting (Eq. 4) are shown in Figure 8. What is interesting, parameters found for P_H mode are identical with these, found in Figure 7. Results of fitting (Eq. 4) confirm that left asymmetric arc from Figure 7 can be interpreted as a result of three separate modes for this temperature.

The same procedure was applied for measurements done for temperatures: 15, 10, 5, 0°C (see Table 2).

The results for temperature 0°C are presented in Figure 9. This fitting does not work well.

It seems that in case of broad X mode it is better to use Cole-Cole [15,16] or Havriliak–Negami [18] fitting. We decided to use for broad X mode arc (from −23°C to −45°C) Cole-Cole fitting procedure (Eq. 5).

$$\varepsilon^*_{LC} = \varepsilon'_{LC} - j\varepsilon''_{LC} = \varepsilon_\infty + \frac{\Delta\varepsilon_{XM}}{1 + \left(jf/f_{RXM}\right)^{1-\alpha}}. \tag{5}$$

Table 2. Results of fitting procedure (4) for five temperatures in SmC_A^* phase

T [°C]	ε_∞	f_{RPH} [kHz]	$\Delta\varepsilon_{PH}$	f_{RXM} [kHz]	$\Delta\varepsilon_{XM}$	f_{RYM} [kHz]	$\Delta\varepsilon_{YM}$	f_{RZM} [kHz]	$\Delta\varepsilon_{ZM}$
20	3.576	10.91	1.46	377.3	1.18	1478.0	1.21	8946.7	0.883
15	3.524	6.037	1.52	236.1	1.79	1213.0	1.14	8640.3	0.783
10	3.473	3.135	1.56	129.8	1.66	829.89	1.16	7878.8	0.741
5	3.477	1.523	1.59	64.652	1.82	543.39	1.14	5738.5	0.681
0	3.409	0.822	1.50	31.897	1.99	338.35	1.12	4837.5	0.671

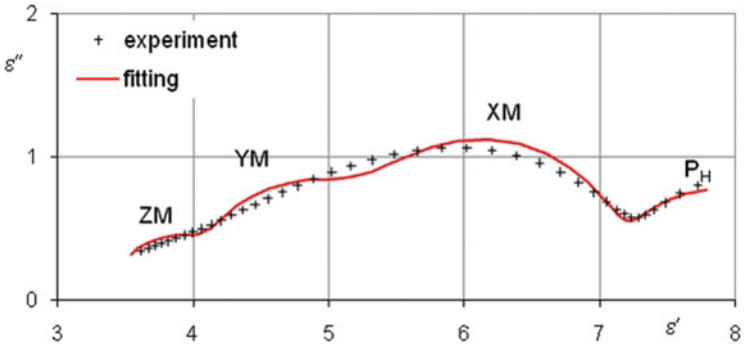

Figure 9. Experimental and fitting results for temperature 0°C, where four modes (P_H, X, Y, Z) are assumed. Found relaxation frequencies: $f_{RPH} = 0.822\,kHz$, $f_{RXM} = 31.90\,kHz$, $f_{RYM} = 338.4\,kHz$, $f_{RZM} = 4837.5\,kHz$; dielectric strengths equal: $\Delta\varepsilon_{PH} = 1.50$, $\Delta\varepsilon_{XM} = 1.997$, $\Delta\varepsilon_{YM} = 1.119$, $\Delta\varepsilon_{ZM} = 0.671$; high frequency limit $\varepsilon_\infty = 3.409$. (Figure appears in color online.)

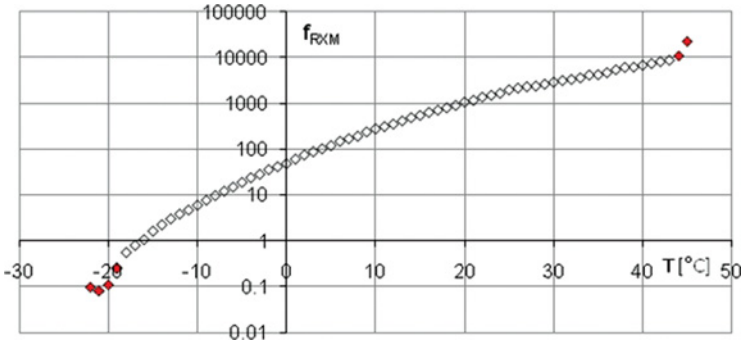

Figure 10. Relaxation frequency (f_{RXM}) found for X mode arc using Cole-Cole model, versus temperature (T). Full diamonds point are doubtful. (Figure appears in color online.)

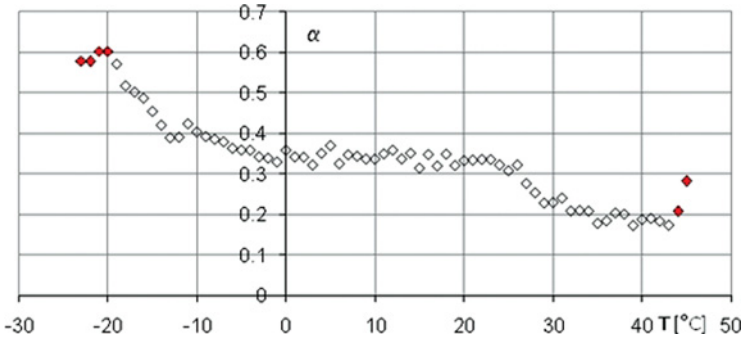

Figure 11. Cole – Cole distribution parameter (α) calculated for X mode arc, versus temperature (T). Full diamonds points are doubtful. (Figure appears in color online.)

Of course in this case we use only the peak of this arc (which is rather symmetric) for fitting. Results are presented in Figures 10 and 11. Where X mode relaxation frequency (f_{RXM}) as well as Cole-Cole distribution parameter (α) are shown versus temperature. The shape of $f_{RXM}(T)$ is exactly the same as it can be read from Figures 2 and 3. Parameter α shows that for higher temperatures ($\sim$40°C) X mode is almost like a mono-Debye type ($\alpha < 0.2$), while for low temperatures (~ -20°C) X mode can be interpreted as a result of a few modes superposition ($\alpha \approx 0.6$). For high ($\sim$45°C) and low (~ -20°C) temperatures it is difficult to determine f_{RXM} and α because it is very close to the measuring limits of experimental setup.

5. Conclusions

Investigated mixture (W-1000) exhibits a very reach spectrum of dielectric modes. Some of them are visible in low temperature, some of them are detected in high temperature SmC_A^* phase. In [7] four possible collective modes, in planar oriented cell are described for SmC_A^*. Two of them are called phasons because they are related to phase angle (ϕ) fluctuations (in somehow they are similar to Goldstone mode in SmC^*). Two of them are called amplitudons because they are related to tilt angle (θ) fluctuations (in somehow they are similar to soft mode in SmA^* and SmC^*). P_L and P_H modes can be interpreted as in-phase and anti-phase phason fluctuations respectively. Modes P_H and P_L can be fitted using one Debye mode. Relaxation frequency of P_L mode is higher than for Goldstone mode. It means that the similar fluctuations (in-phase phasons) in SmC_A^* are faster than in SmC^*. X mode was earlier interpreted [10,11] as anti-phase amplitudon, because it is faster, larger than P_H and P_L and BIAS field influence on X mode is opposite to the influence on P_H and P_L modes.

One can see that situation with X-mode is more complicated. This mode cannot be fitted as one Debye mode. It seems that this arc is created by three modes, called in this paper X, Y and Z. Using Cole-Cole fitting one can notice that Cole-Cole distribution α parameter changes from 0.2 up to 0.6. It confirms that this arc should be explained as an effect of more than one Debye type relaxation or one relaxation calculated from Cole-Cole model.

What about forth, in-phase amplitudon? It seems that modes X, Y and Z could be interpreted as anti-phase amplitudon, in-phase amplitudon and molecular motions (rotation around short molecular axis) respectively.

If this explanation is true, one can propose the new system of collective modes description in SmC_A^*:

P_H mode can be named as P_{ANTI} mode (anti-phase phason), P_L mode can be named as P_{IN} mode (in-phase phason), X mode can be named as A_{ANTI} mode (anti-pase amplitudon), Y mode can be named as A_{IN} mode (in-phase amplitudon).

This is the eutectic mixture. We believe that molecules are well mixed in this mixture and one uniform phase is created in the whole sample. It means that in dielectric response we cannot detect signals from different phases created from different molecules, constituting the mixture.

Another explanation for high frequency modes: X, Y, Z (which create X mode arc) are non-collective modes (at least Y, Z, modes). Such molecular modes (rotation around short molecular axis (S-process) and rotation around long molecular axis (L-process)) can be detected in similar frequency range. Y mode called A_{IN} mode, is very similar to molecular motion around short molecular axis, while Z mode

can be rotation around long molecular axis. Such explanation of high frequency modes in SmC_A^* one can find in [19,20].

Acknowledgment

This work was supported by University project: PBS 23-827/2010/WAT.

References

[1] Lagerwall, S. T., Dahlgren, A., Jägemalm, P., Rudquist, P., D'Havé, K., Pauwels, H., Dąbrowski, R., & Drzewinski, W. (2001). *Advanced Funtional Materials*, *11*, 87.
[2] Dąbrowski, R., Gąsowska, J., Otón, J., Piecek, W., Przedmojski, J., & Tykarska, M. (2004). *Displays*, *25*, 9.
[3] Piecek, W., Raszewski, Z., Perkowski, P., Morawiak, P., Żurowska, M., Ziobro, D., Kula, P., & Sun, X. W. (2009). *MCLC*, *509*, 336.
[4] Różański, S. A., & Thoen, J. (2007). *Liquid Crystals*, *34*, 519.
[5] Pandey, M. B., Dhar, R., Agrawal, V. K., Dąbrowski, R., & Tykarska, M. (2004). *Liquid Crystals*, *31*, 973.
[6] Wojciechowski, M., Bąk, G. W., & Tykarska, M. (2008). *Opto-Electronics Review*, *16*, 257.
[7] Muševič, I., Blinc, R., & Žekš, B. (2000). *The Physics of Ferroelectric and Antiferroelectric Liquid Crystals*, World Scientific, Publishing Co. Pte. Ltd.: Singapore.
[8] Buivydas, M., Gouda, F., Lagerwall, S. T., & Stebler, B. (1995). *Liquid Crystals*, *18*, 879.
[9] Perkowski, P., Piecek, W., Raszewski, Z., Ogrodnik, K., Rutkowska, J., Żurowska, M., Dąbrowski, R., Kędzierski, J., & Sun, X. W. (2008). *Ferroelectrics*, *365*, 88.
[10] Perkowski, P., Raszewski, Z., Piecek, W., Ogrodnik, K., Żurowska, M., Dąbrowski, R., & Sun, X. W. (2009). *MCLC*, *509*, 328.
[11] Perkowski, P., Ogrodnik, K., Piecek, W., Raszewski, Z., Żurowska, M., & Dąbrowski, R. (2010). *MCLC*, *525*, 64.
[12] Perkowski, P. (2009). *Opto-Electronics Review*, *17*, 180.
[13] Perkowski, P. (2011). "Numerical elimination methods of ITO cell contribution to dielectric spectra of ferroelectric liquid crystals", accepted for *Opto-Electronics Review.*
[14] Perkowski, P., Łada, D., Ogrodnik, K., Rutkowska, J., Piecek, W., & Raszewski, Z. (2008). *Opto-Electronics Review*, *16*, 271.
[15] Cole, K. S., & Cole, R. H. (1941). *J. Chem. Phys.*, *9*, 341.
[16] Cole, K. S. & Cole, R. H. (1942). *J. Chem. Phys.*, *10*, 98.
[17] Debye, P. & Physik, Z. (1912). *13*, 97.
[18] Havriliak, S. & Negami, S. (1967). *Polymer*, *8*, 161.
[19] Mikułko, A., Douali, R., Legrand, Ch., Marzec, M., Wróbel, S. & Dąbrowski, R. (2005). *Phase Transitions*, *78*, 949.
[20] Marzec, M., Mikułko, A., Wróbel, S., Haase, W., & Dąbrowski, R. (2005). *MCLC*, *437*, 169.